

## Linear estimation and control of coherent structures in wall-bounded turbulence at $Re_\tau = 2000$

S. F. Oehler and S. J. Illingworth

Department of Mechanical Engineering  
The University of Melbourne, Victoria 3010, Australia

### Abstract

We study the estimation and control problems for a fully-developed turbulent channel flow at  $Re_\tau = 2000$ . A Navier-Stokes-based linear model (which includes an eddy viscosity in the linear operator) is employed to design estimators and feedback controllers. Our study compares a more traditional approach with sensors and actuators placed at the wall to alternative sensors and actuators inside the flow itself. The work is in three parts. First, we consider the optimal estimation problem in which a Kalman filter uses time-resolved measurements at a single wall-normal location (provided by DNS) to estimate the time-resolved velocity field at other wall-normal locations. The estimator reproduces the largest scales with reasonable accuracy for a range of wavenumber pairs, measurement locations and estimation locations; the linear model is also able to predict with reasonable accuracy the performance that will be achieved by the estimator when we apply it to DNS. Second, we consider the full-information control problem where the entire flow field is known; but actuation is at only a single wall-normal location. The linear model predicts that control is most effective when we apply it to the largest, most energetic scales. Third, we consider the input-output control problem with time-resolved measurements at only a single wall-normal location; and actuation at only a single wall-normal location.

### Introduction

This study considers a fully-developed turbulent channel flow at  $Re_\tau = 2000$ . Specifically, it looks at estimating and controlling the largest, most energetic structures of the flow. A linear Navier-Stokes-based model is used to design estimation and control systems which employ sensors and actuators. A particular focus of this work is a comparison of wall-based and in-flow sensing; and a comparison of wall-based and in-flow actuation. It is interesting to know if we should consider in-flow placements over more traditional wall-based ones for potential performance gains. (We only study single-sensor and single-actuator set-ups for simplicity.)

We consider a statistically steady incompressible turbulent channel flow at a friction Reynolds number  $Re_\tau = u_\tau h/\nu = 2000$ , where  $\nu$  is the kinematic viscosity,  $h$  the channel half-height,  $u_\tau = \sqrt{\tau_w/\rho}$  the friction velocity,  $\tau_w$  the wall shear stress, and  $\rho$  the density. Streamwise, spanwise, and wall-normal spatial coordinates are denoted by  $[x, y, z]$  and the corresponding velocities by  $\mathbf{u} = [u, v, w]$ . Spatial variables are normalised by  $h$ , velocities by  $u_\tau$ , time by  $h/u_\tau$  and pressure  $p$  by  $\rho u_\tau^2$ .

### The linear model

A linear model (LM) for the turbulent channel flow is obtained by linearising the Navier-Stokes equations about the mean velocity profile [12, 7]:

$$\begin{aligned} \partial \mathbf{u} / \partial t = & -(\mathbf{U} \cdot \nabla) \mathbf{u} - (\mathbf{u} \cdot \nabla) \mathbf{U} - \nabla p \\ & + \nabla \cdot [v_T / \nu (\nabla \mathbf{u} + \nabla \mathbf{u}^T)] + \mathbf{d}, \end{aligned} \quad (1)$$

where  $\nabla \cdot \mathbf{u} = 0$ ,  $v_T(z)$  is the eddy viscosity profile, and  $\mathbf{d} =$

$-(\mathbf{u} \cdot \nabla) \mathbf{u} + \overline{(\mathbf{u} \cdot \nabla) \mathbf{u}}$  contains all non-linearities. An analytical fit is used [2] for the eddy viscosity profile as in a number of previous studies [12, 4, 9, 7].

$$\begin{aligned} v_T(z) = & 0.5\nu(1 + 3^{-2}\kappa^2 Re_\tau^2(2z - z^2)^2(3 - 4z + z^2)^2 \\ & \times [1 - \exp(-Re_\tau z/A)]^2)^{\frac{1}{2}} + 0.5\nu. \end{aligned} \quad (2)$$

The constants  $\kappa = 0.426$  and  $A = 25.4$  give the best fit to the mean velocity profile at  $Re_\tau = 2003$  [4]. Integrating  $(1 - z)/v_T(z)$  provides the mean velocity profile  $\mathbf{U}$ .

The design of the estimators and controllers to be employed requires a linear time-invariant state-space model. It is achieved by first converting to the Orr-Sommerfeld Squire form and taking Fourier transforms in the homogeneous directions ( $x$  and  $y$ ). We then discretise in the wall-normal direction using Chebyshev collocation of order 200. (Convergence has been checked.) The state-space model at a single wavenumber pair is thus:

$$\dot{\mathbf{x}}(t) = \mathbf{A}\mathbf{x}(t) + \mathbf{B}\mathbf{d}(t), \quad (3a)$$

$$\mathbf{u}(t) = \mathbf{C}\mathbf{x}(t), \quad (3b)$$

where  $\mathbf{x} = [\hat{\mathbf{w}}, \hat{\boldsymbol{\eta}}]^T$  represents the states of the system (wall-normal velocity and vorticity), and  $\mathbf{d} = [\hat{\mathbf{d}}_x, \hat{\mathbf{d}}_y, \hat{\mathbf{d}}_z]^T$  represents all non-linearities. For the linear estimator and controller design, the terms in  $\mathbf{d}$  are treated as random forcing which is white in space and time. The linear dynamics are described by  $\mathbf{A}$ , the forcing is distributed throughout the channel by  $\mathbf{B}$ , and  $\mathbf{C}$  is set to output the flow field of one half of the channel only:

$$\mathbf{A} = \begin{bmatrix} \Delta^{-1} \mathcal{L}_{OS} & 0 \\ -ik_x U' & \mathcal{L}_{SQ} \end{bmatrix}, \quad (4)$$

$$\mathcal{L}_{OS} = ik_x(U''(z) - U(z)\Delta) + v_T \Delta^2 + 2v_T' \mathcal{D} \Delta + v_T'' (\mathcal{D}^2 + k^2),$$

$$\mathcal{L}_{SQ} = -ixU(z) + v_T \Delta + v_T' \mathcal{D},$$

$$\mathbf{B} = \begin{bmatrix} -ik_x \Delta^{-1} \mathcal{D} & ik_y \\ -ik_y \Delta^{-1} \mathcal{D} & -ik_x \\ -k^2 \Delta^{-1} & 0 \end{bmatrix}^T, \quad \mathbf{C} = \frac{1}{k^2} \begin{bmatrix} ik_x \mathcal{D} & -ik_y \\ ik_y \mathcal{D} & ik_x \\ k^2 & 0 \end{bmatrix},$$

where  $\mathcal{D} = \frac{\partial}{\partial z}$ ,  $(\cdot)' = \frac{\partial}{\partial z}(\cdot)$ ,  $k^2 = k_x^2 + k_y^2$ , and  $\Delta = \mathcal{D} - k^2$ . The boundary conditions are:  $\hat{\mathbf{w}}_{wall}(t) = \hat{\mathbf{w}}'_{wall}(t) = \boldsymbol{\eta}_{wall}(t) = 0$ . We quantify the energy of the flow ( $\|\mathbf{u}\|_2 = \mathbf{C}^* \mathbf{X} \mathbf{C}$ ) via the  $H_2$ -norm, where  $\mathbf{X}$  is obtained by solving the following Lyapunov equation:  $\mathbf{A} \mathbf{X} + \mathbf{X} \mathbf{A}^* = -\mathbf{B} \mathbf{B}^*$  [8].

### The Direct Numerical Simulation (DNS) dataset

We employ a DNS dataset provided by the Polytechnic University of Madrid [6, 5]. The homogeneous streamwise and spanwise directions (extending  $8\pi \times 3\pi$ ) are discretised by Fourier expansion (with a spacing of  $\Delta k_x = 1/4$  and  $\Delta k_y = 2/3$ , where  $k$  represents wavenumbers), and the wall-normal direction is discretised using a compact difference scheme of 7th order. The range of wavenumbers (and wavelengths) considered for optimal placement is  $|k_x| \leq 0.5$  ( $|\lambda_x| \geq 12.57$ ) and  $0 < k_y \leq 6$

( $\lambda_y \geq 1.05$ ). Only positive spanwise wavenumbers ( $k_y$ ) are considered, because the data is real-valued in physical space, and therefore the coefficients for modes  $(+k_x, +k_y)$  are the same as those for  $(+k_x, -k_y)$ . Data were saved every  $\delta t = 0.0111$  and terminated at  $t_{max} = 12.72$ . A total of  $t_{max}U_c/(8\pi) = 12.33$  channel flow-throughs ensures that any transients in the estimators and controllers are negligible (where  $U_c$  is the mean velocity at the channel centre). By integrating  $\mathbf{u}$  in time:  $|\mathbf{u}|_2 = [\int_0^{t_{max}} \mathbf{u}^*(t)\mathbf{u}(t)dt]^{1/2}$  we obtain the energy of the DNS flow.

### The estimation problem

In this section, we employ a single measurement to estimate the flow field  $\mathbf{u}$  of the turbulent channel flow. Specifically, we want to compare the performance between two different set-ups. In the first set-up, the sensors are placed inside the flow and would presumably measure velocity  $[u, v, w]$  in a practical application. Measuring all three velocity components might not be feasible. Thus we will investigate which flow direction provides the best estimates. The quality of the estimates will also depend on the location of the sensor inside the flow. The second set-up places sensors at the wall; they would presumably measure shear stress or pressure  $[\tau_x, \tau_y, p]$ . Again, it might not be feasible to measure all three quantities for estimation.

This section is in four parts: (i) we introduce the optimal estimation (OE) problem, (ii) we determine which flow direction is best to measure, (iii) we find the optimal location for the in-flow measurement, and (iv) we compare the estimation-performance of in-flow measurements to wall-based ones in physical space.

Given a measurement  $\mathbf{y}$  at a single wall-normal location  $z_s$ , the task in the OE problem is to estimate the flow field  $\mathbf{u}$ , where the estimate  $\hat{\mathbf{u}}$  is generated using a linear estimator designed to minimise the estimation error  $\mathbf{e} = \mathbf{u} - \hat{\mathbf{u}}$ . The estimation performance is quantified by the normalised  $H_2$ -norm ( $\gamma_{OE}^2 = |\mathbf{e}|_2^2/|\mathbf{u}|_2^2$ ). For more information on the estimator design refer to [11].

The measurement is  $\mathbf{y} = \mathbf{C}_y\mathbf{u} + \mathbf{n}$ , where  $\mathbf{C}_y$  represents the sensor matrix,  $\mathbf{n}$  the sensor noise, and  $\mathbf{u}$  is either provided by the DNS data, which we refer to as DNS-OE, or the LM, which we refer to as LM-OE. The in-flow measurements are:

$$\mathbf{y}|_{\text{flow}} = \begin{bmatrix} \hat{\mathbf{u}}(z = z_s) \\ \hat{\mathbf{v}}(z = z_s) \\ \hat{\mathbf{w}}(z = z_s) \end{bmatrix} + \mathbf{n}, \quad (5)$$

which is achieved using barycentric interpolation. The wall measurements are given by [1]:

$$\mathbf{y}|_{\text{wall}} = \frac{\mathcal{D}}{\text{Re}} \begin{bmatrix} \hat{\mathbf{u}} \\ \hat{\mathbf{v}} \\ \frac{\mathcal{D}^2}{k^2} \hat{\mathbf{w}} \end{bmatrix}_{\text{wall}} + \mathbf{n}, \quad (6)$$

which represent streamwise shear  $\tau_x$ , spanwise shear  $\tau_y$ , and pressure  $p$ .

We generate  $\gamma_{\Sigma OE}$  for each measurement direction ( $[u, v, w]$  and  $[\tau_x, \tau_y, p]$ ), where  $\gamma_{\Sigma OE}$  is the averaged  $H_2$  energy norm for the wavenumbers considered:

$$\gamma_{\Sigma OE}^2 = \frac{\sum_{i \in k_x, j \in k_y} |\mathbf{e}(i, j)|_2^2}{\sum_{i \in k_x, j \in k_y} |\mathbf{u}(i, j)|_2^2}. \quad (7)$$

Streamwise measurements  $u$  for DNS-OE (taken at  $z_s = 0.2$  for now), result in  $\gamma_{\Sigma OE} = 0.54$ , which is 9.1% worse than all three measurements  $[u, v, w]$  taken together at the same location. The streamwise shear measurements  $\tau_x$  result in  $\gamma_{\Sigma OE} = 0.67$ , which is 2.5% worse than taking all three wall-based measurements

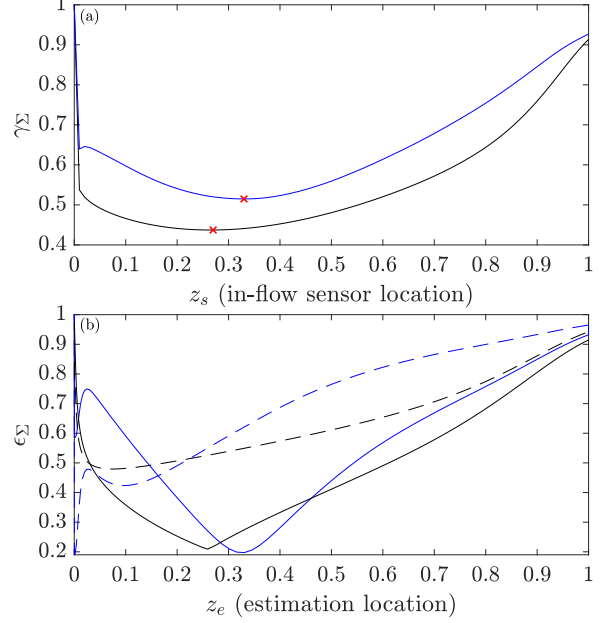


Figure 1: (a) The norm  $\gamma_{\Sigma OE}$  as a function of sensor location  $z_s$  for DNS-OE (—) and LM-OE (—). Optimal locations are indicated (×). (b) The distribution of the estimation error  $\epsilon_{\Sigma}$  when measuring at  $z_{s\text{-opt}}$  or  $z_{s\text{-wall}}$  as a function of estimation location  $z_e$  for DNS-OE ( $u$ (—),  $\tau_x$ (- -)) and LM-OE ( $u$ (—),  $\tau_x$ (- -)).

$[\tau_x, \tau_y, p]$  together. Therefore we choose to only measure  $u$  or  $\tau_x$  as the penalty in performance is acceptable when compared to measuring all three components.

We are now interested in the best in-flow sensor location  $z_{\text{opt}}$  to see the performance difference between wall-based and in-flow sensors. To find  $z_{\text{opt}}$ , we have to either solve  $\gamma_{\Sigma OE}$  for a set of sensor locations  $z_s$ , known as brute force solving or use an iterative gradient minimisation algorithm. We employ the iterative gradient minimisation algorithm by Chen and Rowley [3]. The gradient formulation for LM-OE can be found in [11]. The gradient formulation for the DNS-OE is:

$$\frac{\partial \gamma_{\Sigma OE}}{\partial z_s} = \frac{\gamma_{\Sigma OE}(z_s + \delta z_s) - \gamma_{\Sigma OE}(z_s)}{\delta z_s}, \quad (8)$$

where  $\delta z_s$  is a relatively small perturbation of  $z_s$ , and  $\gamma_{\Sigma OE}$  is generated from time domain simulations. The optimal sensor-location will depend on the wavenumber pairs considered. Therefore we use  $\gamma_{\Sigma OE}$  (7) to find the overall optimal location.

Figure 1a shows  $\gamma_{\Sigma OE}$  over a range of  $z_s$  for DNS-OE and LM-OE. For DNS-OE the best  $\gamma_{\Sigma}$  is 0.51 at  $z_{s\text{-opt}} = 0.33$ , and for LM-OE  $\gamma_{\Sigma}$  it is 0.44 at 0.26. The  $\gamma_{\Sigma}$  results for LM-OE are on average 15% smaller than for DNS-OE. In figure 1b we take the best placement of figure 1a and show the performance throughout the channel by plotting the RMS ( $\epsilon$ ) which is defined as  $\epsilon^2 = \int_0^h \mathbf{e}^2(x)dx$  [11]. We can see that the flow is best estimated at the sensor location while the estimation performance degrades with distance from the wall. For the shear measurement, the best estimation is achieved in the vicinity of the wall.

We confirm the results in the spatial domain by comparing the streamwise velocity perturbations of the DNS data (figure 2a) with its estimate (2b and 2c) in two-dimensional planes ( $z - y$  at  $x = 1.5\pi$ ) at an instance in time ( $tU_c/h = 0.5$ ). The results agree with figure 1 and with previous studies [10]. Both measurement types tend to under-predict near the channel centre. The in-flow measurements tend to over-predict near the channel

wall. A point equidistant to the two sensors shows the estimator's performance with time (figure 2d).

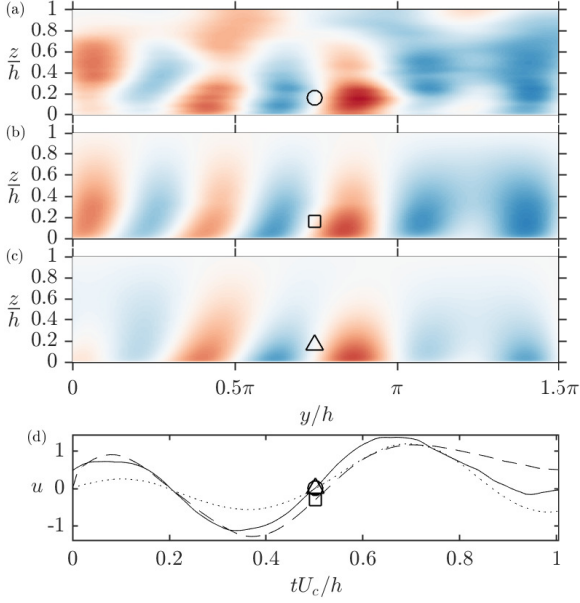


Figure 2: Streamwise velocity perturbations at  $x = 3\pi/2$ : (a) DNS; (b) OE-DNS (in-flow at  $z_{s\text{-opt}} = 0.33$ ); (c) OE-DNS (at wall); and (d) time history at  $y = 3\pi/4$  and  $z = 0.165$  ( $\circ$ ,  $\square$ ,  $\triangle$ ) for DNS reference (—), the in-flow estimate (---), and the wall-based estimate ( $\cdots$ ). Sixty-five contour levels are shown from  $u = -2.5$  (blue) to  $u = 2.5$  (red).

### The full-state information control problem

In this section, we employ a single actuator to reduce perturbations in the entire flow field  $\mathbf{u}$  of the turbulent channel flow which is known as full information control (FIC). Currently, it is impractical to run control studies at  $Re_\tau = 2000$ , and therefore we look at results for the linear model (LM) only. We consider LM-FIC because it predicts the control behaviour of both numerical simulations and experiments [9] and can serve as a benchmark for single-actuator control. Similar to the estimation study, we want to compare an in-flow single-actuator control set-up with a wall-based set-up. The in-flow actuation would presumably be a body force applied in either the streamwise, spanwise, or wall-normal direction and performance will vary with the placement location. The wall-based actuation could either be applied using the Dirichlet or Neumann boundary conditions.

This section is in four parts: (i) we introduce the full-information control (FIC) problem, (ii) we determine the best flow direction to actuate in, (iii) we find the optimal location for the in-flow actuator, (iv) we present results in physical space.

Given knowledge of the entire flow field  $\mathbf{u}$ , the task in the full-state information control (FIC) problem is to control the flow field  $\mathbf{u}$  using an actuator at a single wall-normal location  $z_a$ . The actuator force is generated by a controller designed to minimise the magnitude of  $\mathbf{u}$ . The control performance is quantified by the  $H_2$ -norm  $\gamma_{FI} = \|\mathbf{u}\|_2 / \|\mathbf{u}_{\text{ref}}\|_2$ , where  $\mathbf{u}_{\text{ref}}$  is the uncontrolled reference flow field. For more information on the controller design refer to [11].

The in-flow body forces ( $[\hat{f}_x, \hat{f}_y, \hat{f}_z]$ ) enter the flow in the same way as the random forcing ( $[\hat{\mathbf{d}}_x, \hat{\mathbf{d}}_y, \hat{\mathbf{d}}_z]$ ) by employing barycentric interpolation  $\mathbf{B}(z = z_a)$ . Wall-based actuation

is applied by modifying the boundary condition at the wall  $[\hat{\mathbf{w}}_{\text{wall}}, \hat{\mathbf{w}}'_{\text{wall}}, \eta_{\text{wall}}]$  [1]. As in the estimation problem, we initially place the in-flow actuator at  $z_a = 0.2$  and the wall-mounted actuator at  $z_{a\text{-wall}}$  to generate an averaged  $H_2$  energy norm  $\gamma_{\Sigma FI}$  over the set of wave-number pairs. Actuating  $f_z$  inside the flow results in the best control performance of  $\gamma_{\Sigma FI} = 0.42$ , which is 14.9% larger than actuating all three  $[f_x, f_y, f_z]$  together. We choose to actuate  $d_z$  by itself. The most effective boundary condition to control is  $\hat{\mathbf{w}}_{\text{wall}}$  ( $\gamma_{\Sigma FI} = 0.52$ ) which is unsteady blowing/suction with zero net mass flux [1].

We find the best in-flow actuator location with the same iterative gradient minimisation we used for OE. The gradient formulation for the FIC performance can be found in [11]. The optimal actuator location is at  $z_{a\text{-opt}} = 0.31$  with  $\gamma_{\Sigma FI} = 0.42$ , which is 19.5% lower than the blowing and suction set-up. In figure 3 we show the RMS of the controlled flows along with the uncontrolled reference throughout the channel. In all three cases, the RMS shows the effect of individual disturbances on the norm. For the in-flow case the strongest disturbances are controlled the best and for the wall-based case control is most effective on disturbances near the wall.

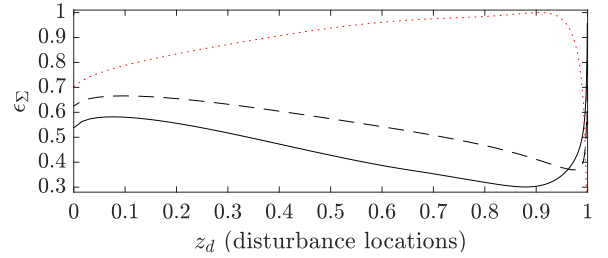


Figure 3: The RMS  $\varepsilon_{\Sigma FI}$  for LM-FIC when actuating at  $z_{a\text{-opt}}$  (—) (in-flow) or  $z_{a\text{-wall}}$  (---) as a function of disturbance location  $z_d$ . The normalised RMS  $\varepsilon_{\Sigma LM}$  for the LM as a function of disturbance location  $z_d$  ( $\cdots$ ).

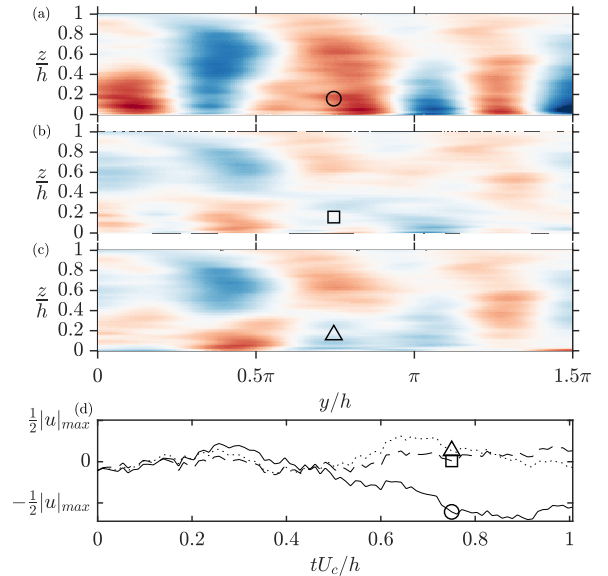


Figure 4: Streamwise velocity perturbation at  $x = 3\pi/2$ : (a) uncontrolled LM reference; (b) LM-FIC (in-flow at  $z_a = 0.31$ ); (c) LM-FIC (at wall with zero-mass flux suction and blowing); and (d) time history at  $y = 3\pi/4$  and  $z = 0.155$  for the reference (—), the in-flow (---), and the wall-based ( $\cdots$ ) case. Sixty-five contour levels are shown from  $-|u|_{\text{max}}$  (blue) to  $|u|_{\text{max}}$  (red).

We now look at the results in the spatial domain by comparing the streamwise velocity perturbations generated from the linear model (figure 4a) with the controlled flows (figures 4b and 4c) in two-dimensional planes ( $z - y$  at  $x = 1.5\pi$ ) at an instance in time ( $tU_c/h = 0.5$ ). As expected, the in-flow actuator performs better than the wall-mounted actuator. We can see that the process of suction and blowing can introduce strong velocity perturbations at the wall. In figure 4d we consider a point equidistant between the wall-based and in-flow actuator. We can see that the actuators reduce the perturbations significantly at that location. The lines in all four figures are noisy due to the constant application of random disturbances everywhere.

### The input-output control problem

Now we want to compare the FIC problem to the input-output control (IOC) problem, which is the FIC problem without knowledge of the entire flow field  $\mathbf{u}$ . IOC is more practical than FIC because the entire state of the flow is usually unknown. Instead of the entire state, the controller uses an estimate  $\mathbf{u}'$  which is generated by the optimal estimator via measurements of either  $u$  or  $\tau_x$ . (Hence, IOC uses a single sensor and a single actuator.) We initially studied the FIC problem, because it eliminates the challenges of having measurements (limited to a single location). FIC isolates the challenges of actuation (limited to a single location) and therefore provides a benchmark for single-actuator control.

In Figure 5 we compare the energy norms of the LM-OE, LM-FIC and LM-IOC problems over a range of  $k_y$  (we average  $|k_x| \leq 0.5$ ) with sensors and actuators placed at the optimal locations. All performances are best at  $k_y \approx 1.9$ , which is where the flow is most amplified by disturbances [12]. The FIC and IOC performance results are similar to each other. In IOC, we can only control perturbations which are known to the controller. Therefore, the perturbations which can be controlled well must also be captured by the sensor. We have included the energy norms of the LM-OE problem, which are shown to be always lower than for the LM-IOC problem.

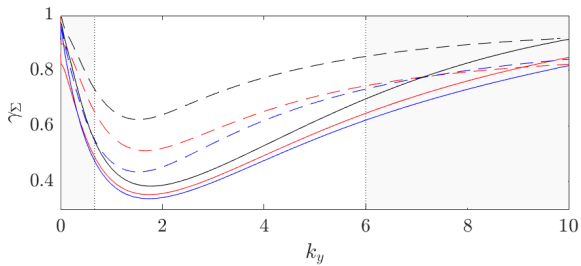


Figure 5: The norm  $\gamma_\Sigma$  averaged over  $k_x \leq 0.5$  as a function of  $k_y$  for OE-LM ( $u$  (—),  $\tau_x$  (---)), for FIC-LM ( $u$  (—),  $\tau_x$  (---)), and for IOC-LM ( $u$  (—),  $\tau_x$  (---)). The range of  $k_y$  considered for optimal placement is marked white.

### Discussion and conclusion

We studied estimation and control for a turbulent channel flow using single-sensor and single-actuator set-ups. Specifically, we compared the performance between in-flow and wall-based set-ups. For the OE and IOC problems, we measured velocity or shear in the streamwise direction only. For the FIC and IOC problems, we applied a body force or blowing & suction in the wall-normal direction only. [8].

Table 1 provides a summary of the results for OE with DNS and LM measurements, and also FIC and IOC applied to the linear model. The table shows the best performance achieved by wall-based and optimal in-flow placements. It also shows

	DNS-OE	LM-OE	LM-FIC	LM-IOC
$\gamma_\Sigma$ (at wall)	0.6718	0.5915	0.5204	0.6931
$\gamma_\Sigma$ (in-flow)	0.5148	0.4372	0.4188	0.4712
$z_{s\text{-opt}}(u)$	0.3295	0.2712		0.2587
$z_{a\text{-opt}}(d_z)$			0.3076	0.2931

Table 1: Summary of results

the sensor and actuator locations where the best in-flow performance is achieved. For all set-ups, the in-flow placement provides better performance than the wall-based placement. Figure 1 shows that the performance of DNS-OE degrades more rapidly with distance from the sensor location than the performance of LM-OE which results in a 15% smaller  $\gamma_{\Sigma OE}$  for LM-OE. Nevertheless, LM-OE still finds a location close to the optimal DNS-OE sensor location. At this location DNS-OE achieves  $\gamma_{\Sigma OE}(z_s = 0.2712) = 0.5199$ , which is 1% larger than  $\gamma_{\Sigma OE}(z_s = 0.3295)$ . In the future, it would be interesting to implement FIC and IOC to the channel flow in DNS.

### References

- [1] Bewley, T. R. and Liu, S., Optimal and robust control and estimation of linear paths to transition, *J. Fluid Mech.*, **365**, 1998, 305–349.
- [2] Cess, R. D., *A survey of the literature on heat transfer in turbulent tube flow*, Westinghouse Research, 1958.
- [3] Chen, K. K. and Rowley, C. W.,  $H_2$  optimal actuator and sensor placement in the linearised complex Ginzburg-Landau system, *J. Fluid Mech.*, **681**, 2011, 241–260.
- [4] del Alamo, J. C. and Jiménez, J., Linear energy amplification in turbulent channels, *J. Fluid Mech.*, **559**, 2006, 205–213.
- [5] Encinar, M. P., Vela-Martín, A., García-Gutiérrez, A. and Jiménez, J., A second-order consistent, low-storage method for time-resolved channel flow simulations, *arXiv preprint: flu-dyn/1808.06461*, 2018.
- [6] Hoyas, S. and Jiménez, J., Scaling of the velocity fluctuations in turbulent channels up to  $Re\tau=2003$ , *Phys. Fluids*, **18**, 2006, 1–4.
- [7] Illingworth, S. J., Monty, J. P. and Marusic, I., Estimating large-scale structures in wall turbulence using linear models, *Journal of Fluid Mechanics*, **842**, 2018, 146–162.
- [8] Jovanović, M. R. and Bamieh, B., Componentwise energy amplification in channel flows, *J. Fluid Mech.*, **534**, 2005, 145–183.
- [9] Moarref, R. and Jovanović, M. R., Model-based design of transverse wall oscillations for turbulent drag reduction, *J. Fluid Mech.*, **707**, 2012, 205–240.
- [10] Oehler, S., Garcia-Gutiérrez, A. and Illingworth, S., Linear estimation of coherent structures in wall-bounded turbulence at  $Re_\tau = 2000$ , *J. Phys. Conf. Ser.*, **1001**, 2018, 012006.
- [11] Oehler, S. F. and Illingworth, S. J., Sensor and actuator placement trade-offs for a linear model of spatially developing flows, *J. Fluid Mech.*, **854**, 2018, 34–55.
- [12] Pujals, G., García-Villalba, M., Cossu, C. and Depardon, S., A note on optimal transient growth in turbulent channel flows, *Phys. Fluids*, **21**, 2009, 015109.